Roles of noise in single and coupled multiple genetic oscillators

Mitsumasa Yoda
Department of Computational Science and Engineering, Nagoya University, Nagoya 464-8603, Japan

Tomohiro Ushikubo
Department of Computational Science and Engineering, Nagoya University, Nagoya 464-8603, Japan and Graduate School of Human Informatics, Nagoya University, Nagoya 464-8601, Japan

Wataru Inoue
Department of Complex Systems Science, Nagoya University, Nagoya 464-8601, Japan

Masaki Sasai
Department of Computational Science and Engineering, Nagoya University, Nagoya 464-8603, Japan; Graduate School of Human Informatics, Nagoya University, Nagoya 464-8601, Japan; Department of Complex Systems Science, Nagoya University, Nagoya 464-8601, Japan; and CREST-Japan Science and Technology Agency, Nagoya 464-8603, Japan

(Received 25 August 2006; accepted 16 January 2007; published online 15 March 2007)

The noisy fluctuation of chemical reactions should profoundly affect the oscillatory dynamics of gene circuit. In this paper a prototypical genetic oscillator, repressilator, is numerically simulated to analyze effects of noise on oscillatory dynamics. The oscillation is coherent when the protein number and the rate of the DNA state alteration are within appropriate ranges, showing the phenomenon of coherence resonance. Stochastic fluctuation not only disturbs the coherent oscillation in a chaotic way but also destabilizes the stationary state to make the oscillation relatively stable. Bursting in translation, which is a source of intense stochastic fluctuation in protein numbers, suppresses the destructive effects of the finite leakage rate of protein production and thus plays a constructive role for the persistent oscillation. When multiple repressilators are coupled to each other, the cooperative interactions among repressilators enhance the coherence in oscillation but the dephasing fluctuation among multiple repressilators induces the amplitude fluctuation in the collective oscillation. © *2007 American Institute of Physics*. [DOI: 10.1063/1.2539037]

I. INTRODUCTION

Since cells are mesoscopic objects and the numbers of biomolecules in each cell are small, the large stochastic fluctuations are expected in chemical reactions in cells. Such intrinsic stochasticity has been quantitatively confirmed by the recent advance in biotechnology: Artificially designed gene circuits have been embedded in bacteria, which provided detailed data on fluctuations of gene expression in individual cells.[1–6] In order to control such stochastic fluctuations and to design the innovative gene circuits, analyses of theoretical models are necessary.[6–8] Theoretical models of several simple circuit motifs such as one-gene switches of positive[9,10] or negative[11,12] feedback and two-gene toggle switches[10,13–17] have been studied intensively. By taking into account both the intrinsic noise arising from the stochastic transcriptional and translational processes and the extrinsic noise arising from cell growth and division, theoretical models have become able to produce data which can be quantitatively compared with experiments.[7] Through such cooperation between experiments and theories, many important factors which influence the stochasticity of gene expression have been elucidated: The typical number of protein molecules, the leakage rate of protein production when the gene expression is repressed, bursts in translation, the number of copies of plasmids, and the difference between the time scale of the DNA state change and that of the protein number fluctuation are a few examples.[8]

Further interesting questions are on circuits which exhibit time-dependent oscillation: In order to design the oscillatory circuits and to analyze the oscillatory behaviors of circuits in genome, we would like to know how the noise affects the oscillatory dynamics. In this paper a prototypical genetic oscillator, repressilator,[1] is studied as an example system, and necessary conditions for the persistent oscillation are discussed.

Among those factors which influence the stochasticity, we pay close attention to the difference between the time scale of the DNA state change and that of the protein number fluctuation. The rate of protein production is changed by the DNA state, and the DNA state is regulated by the protein concentration in cytoplasm. In this way gene switches interact with proteomic atmosphere. Sasai and Wolynes pointed out[18] that this interaction resembles that of the Kondo effect or the electron-transfer reaction in condensed matter. In those problems in condensed matter, difference in speed of change in different constituents of the system profoundly affects the dynamical feature of the whole system. Likewise, the difference in time scale should be important in the dynamical performance of the gene circuit. Binding of regulating proteins to DNA takes place in one cellular compartment in prokary-

ote and should be faster than the complex processes of protein synthesis. Because of this time scale difference, the DNA state in many theoretical models has been treated as in equilibrium reached before the other slow kinetic events proceed.[10] Borrowing the wording from the condensed matter theories, we may call this situation the "adiabatic" situation.[9,11,17] Recent theoretical analyses on the gene switching dynamics, however, showed that even when the assumption of adiabatic situation is adequate to describe the steady state, adiabaticity may not be extremely strong in actual cells and that the effects beyond the adiabatic limit have to be explicitly taken into account to treat kinetics of switching in a correct way.[9] In such "weakly adiabatic" case, the explicit stochastic dynamics of the DNA state change influences the fluctuation of the number of protein molecules and hence should strongly affect the performance of dynamically oscillating gene circuit. In eukaryotes the DNA state change is much slower than in prokaryotes, and the nonadiabatic effects should be even more significant.[19,20]

We define adiabaticity ω by the ratio of the rate of change in the status of the promoter site in DNA to the rate of change in the protein number. When $\omega \gg 1$, the regulating protein binds to or unbinds from DNA so frequently that the fluctuating DNA state can be approximated by its adiabatic equilibrium. When $\omega \ll 1$, on the other hand, the protein number is equilibrated in each DNA state and is altered by following the infrequent DNA switching. In the crossover regime of $\omega \approx 1$, the protein number change should be most nontrivial. When $\omega \approx 10^1 - 10^2$, the stationary state may be described as in the adiabatic limit of $\omega \gg 1$, but the gene switching dynamics is strongly influenced by the nonequilibrium DNA state fluctuation.[9] In this paper the stochastic dynamics of repressilator is numerically simulated with the Gillespie algorithm[21] and is analyzed through the windows of two parameters, ω and X, where X is the typical number of protein molecules in a cell, which is another important factor to influence the stochasticity.

We also analyze the effects of other factors such as the leakage of the protein production when the promoter is occupied by a repressor. Bursting production of proteins at the time of translation also gives rise to a large noisy fluctuation.[6,22] Extrinsic noise arising from the cell division may influence the coherence in oscillation.[7] The last factor we will examine is the number of copies of plasmids. In a usual experimental setup multiple copies of plasmids are embedded in a bacterium cell, and we may expect that the noise amplitude should be decreased when multiple copies of gene circuits work in a cooperative way. We analyze the collective dynamics of coupled multiple repressilators with numerical simulation.

In the next section the model of repressilator is explained. The stochastic reaction kinetics in the model is numerically simulated and the degree of coherence in oscillation is measured by defining "phase coherence." Phase coherence is calculated in a wide range of parameters, and the necessary conditions for the coherent oscillation are looked for. These exact numerical results are compared with the mean-field description of the model. The lowest order treatment in the mean-field description is based on the assumption that the noise effects are minimal, so that differences between the exact numerical results and the lowest order mean-field treatment highlight the importance of the noise effects in oscillation. Coupled multiple repressilators are simulated, and the correlation among repressilators and the resultant collective dynamics are analyzed. The last section is devoted to the summary and discussion.

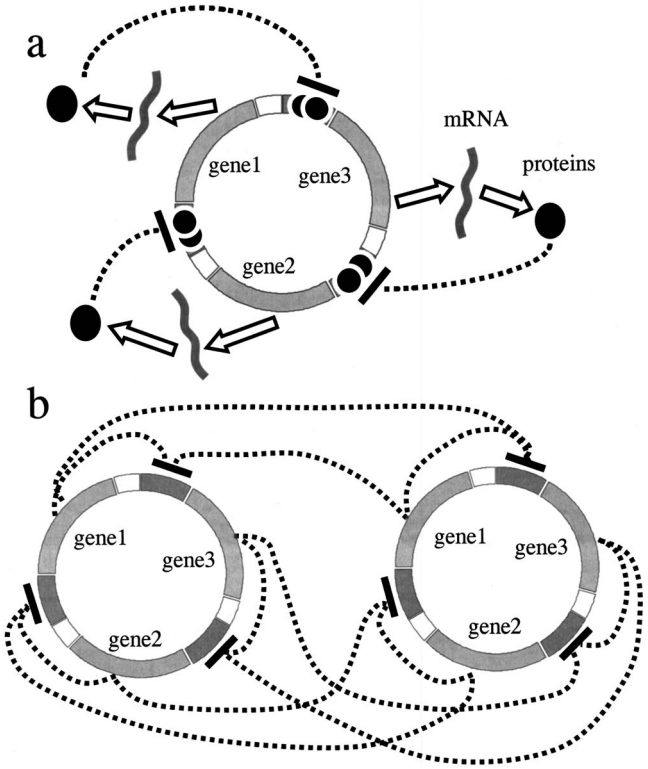

FIG. 1. The model of the repressilator. (a) A repressilator is a circuit composed of three genes, in which one gene represses another gene cyclically. (b) Two repressilators interact through diffusive proteins.

II. MODEL

Repressilator is a circuit composed of three genes, in which a protein synthesized from one gene represses expression of the other gene cyclically, as shown in Fig. 1. Elowitz and Leibler have embedded this circuit in *E. coli* and have shown that it indeed works as an oscillator.[1] This circuit has been used as a prototypical model of gene oscillator in experimental[4] and theoretical[23–25] investigations and in studies of cell-cell communication.[26] As shown in Fig. 1, each gene produces a mRNA, and a mRNA produces a repressor protein. Repressor protein represses the expression of the other gene in a cyclic way. Also shown in Fig. 1 is the case where two identical copies of plasmids are interacting in a cell. Proteins produced from each plasmid are mixed in the cell to bind to the other plasmid. Here, we write $S_{i,p}=1$ or "the DNA state of the ith gene in the pth copy of plasmid is on" when the promoter does not bind the repressor protein and $S_{i,p}=0$ or "the DNA state is off" when the promoter is occupied with the bound repressor protein. Then, the chemical kinetics of change in the DNA state of the ith gene should be

$$S_{i,p} = 1 \underset{f}{\overset{h(n_j)}{\rightleftarrows}} S_{i,p} = 0, \tag{1}$$

where $h(n_j)$ is the rate of binding of the repressor synthesized from the jth gene to the promoter site of the ith gene, $j=3$, 1, and 2 for $i=1$, 2, and 3, respectively. We assume that each repressor acts as a dimer and that the rate of dimerization is fast enough. Then, the binding rate can be written as $h(n_j)=h_0 n_j(n_j-1)$, where n denotes the number of protein molecules. Here, we do not specify n by the plasmid index p under the assumption that proteins quickly diffuse and are mixed in the cell. Proteins may diffuse over the entire prokaryote cell within seconds, which justifies this assumption.[27] f is the rate of unbinding of the repressor from the promoter. In this way the gene switch represented by the two-state variable, $S_{i,p}$, interacts with the proteomic atmosphere of $\{n_i\}$. mRNA is synthesized with the rate γ_s as

$$m_{i,p} \xrightarrow{\gamma_s} m_{i,p} + 1. \tag{2}$$

where $m_{i,p}$ is the number of mRNA molecules produced from the ith gene of the pth plasmid. $\gamma_s=\gamma_1$ when $S_{i,p}=1$ and $\gamma_s=\gamma_0$ when $S_{i,p}=0$ with $\gamma_1 \gg \gamma_0$. mRNA molecules are degraded with the rate $\lambda m_{i,p}$ as

$$m_{i,p} \xrightarrow{\lambda m_{i,p}} m_{i,p} - 1. \tag{3}$$

By writing $m_i=\Sigma_p m_{i,p}$, protein molecules are synthesized with the rate gm_i as

$$n_i \xrightarrow{gm_i} n_i + 1 \tag{4}$$

and are degraded with the rate kn_i as

$$n_i \xrightarrow{kn_i} n_i - 1. \tag{5}$$

See Fig. 2 for the illustrative explanation of kinetics. Because our focus is on the physical mechanism of how the repressilator shows coherent oscillation but not on the detailed comparison with the experimental results, we assume for the sake of simplicity that h_0, f, γ, λ, g, and k are independent of i or p.

Instead of the bare parameters which appeared in Eqs. (1)–(5), we use the normalized ones in the simulation: $\omega=f/k$ is adiabaticity which measures the relative speed of the DNA state change to the speed of the protein number change, $X^{\mathrm{eq}}=f/h_0$ determines the probability that the DNA state is on, $X^m=(\gamma_1+\gamma_0)/(2\lambda)$ is a typical number of mRNA molecules per one plasmid, $\delta X^m=(\gamma_1-\gamma_0)/(\gamma_1+\gamma_0)$ is the relative difference of X^m in on and off states, and $X=KX^m g/k$ is a typical number of protein molecules, where K is the number of copies of plasmid.

A lifetime of proteins should be about the duration of a cell cycle or less, so that we estimate $k \sim 10^{-2}-10^{-3}$ s^{-1}. The degradation of mRNA should be faster than proteins as $\lambda \sim 10^{-1}-10^{-2}$ s^{-1}. Using the data of λ phage,[28] $h_0 \sim 10^{-2}-10^{-7}$ s^{-1} and $f \sim 1-10^{-3}$ s^{-1}, so that ω should be

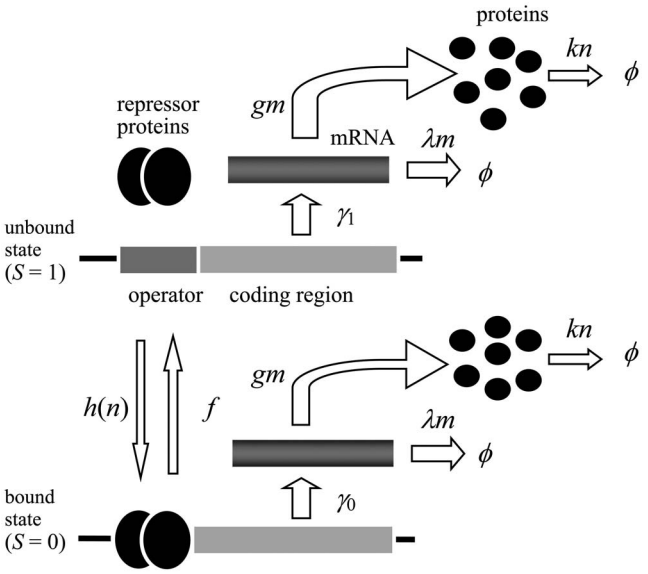

FIG. 2. The scheme of gene expression in the model. mRNA is synthesized with the rate $\gamma_1>0$ when $S_{i,p}=1$ and the rate of mRNA synthesis, γ_0, is zero or much smaller than γ_1 when $S_{i,p}=0$. mRNA is degraded with the rate $\lambda m_{i,p}$. Protein is synthesized with the rate $gm_i=g\Sigma_p m_{i,p}$. Protein is degraded with the rate kn_i. The binding rate of the jth repressor to the promoter of the ith gene is $h_0 n_j(n_j-1)$ with $j=3$, 1, and 2 for $i=1$, 2, and 3, respectively, and the rate of unbinding of the repressor from the promoter is f.

$\omega \sim 10^{-1}-10^{3}$. $X^{\mathrm{eq}}=f/h_0 \sim 10^{2}-10^{4}$ and we use a typical value of $X^{\mathrm{eq}}=10^3$. The typical protein number may be $X \sim 10^0-10^3$, but the typical mRNA number should be $X^m \sim 10^{-1}-10^1$. The leakage production rate of mRNA in the DNA off state should not be very large, so that we examine the range of $1-\delta X^m \sim 0-0.2$.

We also analyze repressilator with the mean-field treatment. The stochastic processes of Eqs. (1)–(5) are described by the joint probability distribution $P(\{S_{i,p}\},\{m_{i,p}\},\{n_i\})$, which represents the probability that the DNA states are $\{S_{i,p}\}$, the mRNA numbers are $\{m_{i,p}\}$, and the protein numbers are $\{n_i\}$. Equations (1)–(5) are expressed by a master equation for $P(\{S_{i,p}\},\{m_{i,p}\},\{n_i\})$. The first order moments are defined by $C_{i,p}=\Sigma_{(S,m,n)} S_{i,p} P(\{S_{i,p}\},\{m_{i,p}\},\{n_i\})$, $M_{i,p,1}C_{i,p}=\Sigma_{(S,m,n)} m_{i,p} S_{i,p} P(\{S_{i,p}\},\{m_{i,p}\},\{n_i\})$, $M_{i,p,0}(1-C_{i,p})=\Sigma_{(S,m,n)} m_{i,p}(1-S_{i,p}) P(\{S_{i,p}\},\{m_{i,p}\},\{n_i\})$, and $N_i=\Sigma_{(S,m,n)} n_i P(\{S_{i,p}\},\{m_{i,p}\},\{n_i\})$, where $\Sigma_{(S,m,n)}$ represents a summation over $\{S_{i,p}\}$, $\{m_{i,p}\}$, and $\{n_i\}$. When we write equations for the first order moments, those equations include the second or higher order moments. The lowest order mean-field equation is obtained by truncating this hierarchy at the first order moment by imposing $\Sigma_{S,m,n}(n_i)^2 P(\{S_{i,p}\},\{m_{i,p}\},\{n_i\})=N_i+N_i^2$, etc. This truncation is equivalent to making the assumption that the protein numbers and the mRNA numbers obey Poisson distributions, which are distributions realized when the noise effects are minimal. Thus, the deviation of the exact numerical results from the lowest order mean-field results of the model highlights the effects of stochastic fluctuation beyond the Poisson distribution. The lowest order mean-field equation has the form

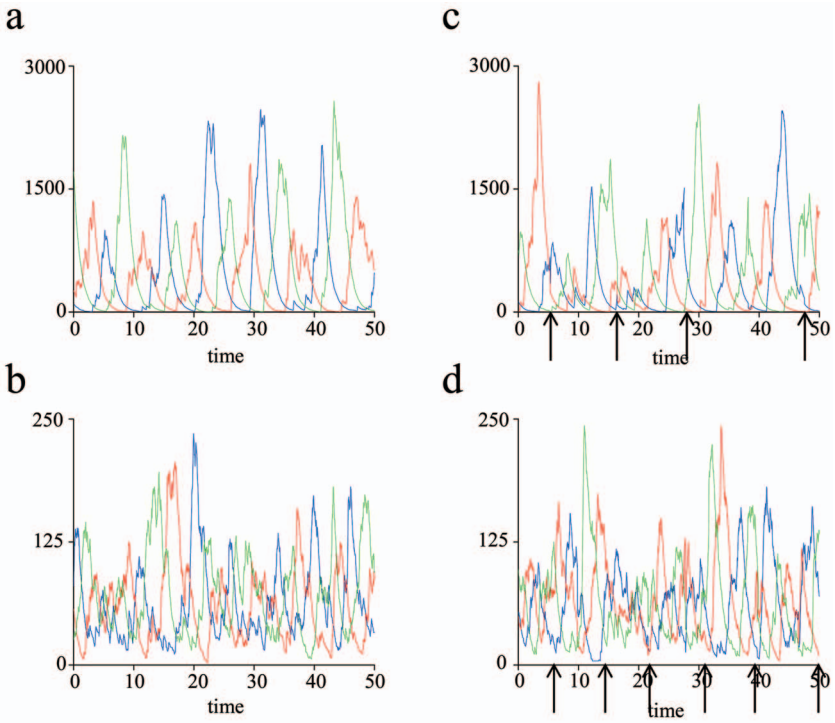

FIG. 3. (Color) Examples of simulated trajectories of a single repressilator of $K=1$. The trajectory represents the temporal change of n_1 (red), n_2 (green), and n_3 (blue). Time in the horizontal axis is measured in units of k^{-1}. $X^m=1$, $1-\delta X^m=0$, and $X^{\mathrm{eq}}=10^3$. (a) $\omega=10^3$ and $X=10^3$ and (b) $\omega=10^3$ and $X=10^2$. Cell division is not explicitly considered in simulations of (a) and (b). (c) $\omega=10^3$ and $X=10^3$ and (d) $\omega=10^3$ and $X=10^2$. Cell division is explicitly considered in (c) and (d) with $T_{\mathrm{cell}}=10$ and $\sigma_{\mathrm{cell}}^2=3$. Cell was divided into two daughter cells at time designated by arrows.

$$\frac{1}{k}\frac{dC_{i,p}}{dt}=\omega\left((1-C_{i,p})-\frac{N_j^2}{X^{\mathrm{eq}}}C_{i,p}\right),$$

$$\frac{1}{\lambda}\frac{d}{dt}\left(\frac{M_{i,p,1}}{X^m}C_{i,p}\right)=\left(1+\delta X^m-\frac{M_{i,p,1}}{X^m}\right)C_{i,p}+\frac{k\omega}{\lambda}\left(\frac{M_{i,p,0}}{X^m}(1-C_{i,p})-\frac{N_j^2}{X^{\mathrm{eq}}}\frac{M_{i,p,1}}{X^m}C_{i,p}\right),$$

$$\frac{1}{\lambda}\frac{d}{dt}\left(\frac{M_{i,p,0}}{X^m}(1-C_{i,p})\right)=\left(1-\delta X^m-\frac{M_{i,p,0}}{X^m}\right)(1-C_{i,p})-\frac{k\omega}{\lambda}\left(\frac{M_{i,p,0}}{X^m}(1-C_{i,p})-\frac{N_j^2}{X^{\mathrm{eq}}}\frac{M_{i,p,1}}{X^m}C_{i,p}\right),$$

$$\frac{1}{k}\frac{d}{dt}\left(\frac{N_i}{X}\right)=\frac{1}{NX^m}\sum_{p=1}^{N}\left(M_{i,p,1}C_{i,p}+M_{i,p,0}(1-C_{i,p})\right)-\frac{N_i}{X}. \tag{6}$$

Defining the expectation value of the mRNA number by $M_{i,p}=M_{i,p,1}C_{i,p}+M_{i,p,0}(1-C_{i,p})$, the deterministic equation for the chemical kinetics of Eqs. (1)–(5) is derived from Eq. (6) as

$$\frac{1}{k}\frac{dC_{i,p}}{dt}=\omega\left((1-C_{i,p})-\frac{N_j^2}{X^{\mathrm{eq}}}C_{i,p}\right),$$

$$\frac{1}{\lambda}\frac{d}{dt}\left(\frac{M_{i,p}}{X^m}\right)=1+\delta X^m C_{i,p}-\delta X^m(1-C_{i,p})-\frac{M_{i,p}}{X^m},$$

$$\frac{1}{k}\frac{d}{dt}\left(\frac{N_i}{X}\right)=\frac{1}{NX^m}\left(\sum_{p=1}^{N}M_{i,p}\right)-\frac{N_i}{X}. \tag{7}$$

In this way Eq. (6) includes Eq. (7), or the lowest order mean-field equation is just a least extension of the deterministic equation. Meanings of the normalized parameters ω, X^{eq}, X^m, and X are visible in Eq. (7): In the adiabatic limit of $\omega\gg 1$, the left hand side of the first equation of Eq. (7) can be neglected, leading to $C_{i,p}=X^{\mathrm{eq}}/(X^{\mathrm{eq}}+N_j^2)$. In this way X^{eq} controls the probability of the DNA state to be on. When we put $C_{i,p}=1/2$ in Eq. (7), we have the stationary solution of $m_{i,p}=X^m$ and $n_i=X$.

III. PHASE COHERENCE

A. Coherent and incoherent oscillations

We first examine a single isolated repressilator of $K=1$ and coupled multiple repressilators of $K=10$ by numerically simulating the processes given in Eqs. (1)–(5) with the Gillespie algorithm. Extrinsic noise is taken into account by considering the cell division process explicitly. We first determine the timing of cell division by assuming that the duration of a cell cycle fluctuates with the Gaussian distribution of an average T_{cell} and a variance σ_{cell}.[2] Then, at this timing of cell division in the simulation, proteins, mRNAs, and plasmids are handed to daughter cells by assuming that n_i, $m_{i,p}$, and the number of the repressor-bound promoters are distributed with the binomial distribution of the equal probability to each of two daughter cells.

Figures 3 and 4 show examples of the simulated temporal change of protein numbers n_1, n_2, and n_3. In Figs. 3(a), 3(c), 4(a), and 4(c) the abundance of proteins is characterized by $X=10^3$, and we can see that three proteins change their numbers, alternatively keeping the coherent ordering of protein synthesis. In Figs. 3(b), 3(d), 4(b), and 4(d) with less

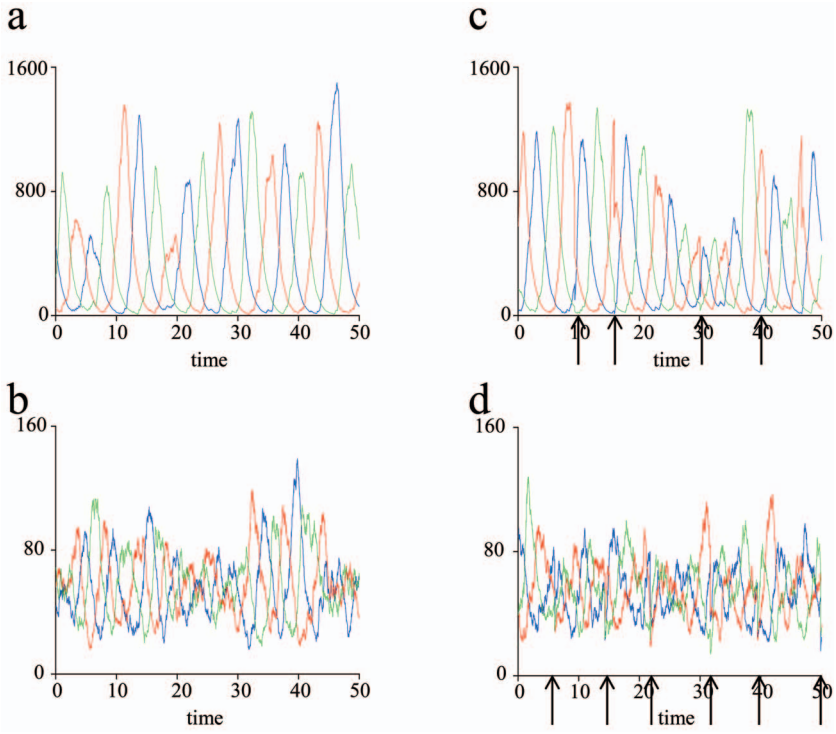

FIG. 4. (Color) Examples of simulated trajectories of multiply coupled repressilators of $K=10$. The trajectory represents the temporal change of n_1 (red), n_2 (green), and n_3 (blue). Time in the horizontal axis is measured in units of k^{-1}. $X^m=1$, $1-\delta X^m=0$, and $X^{\mathrm{eq}}=10^3$. (a) $\omega=10^3$ and $X=10^3$ and (b) $\omega=10^3$ and $X=10^2$. Cell division is not explicitly considered in simulations of (a) and (b). (c) $\omega=10^3$ and $X=10^3$ and (d) $\omega=10^3$ and $X=10^2$. Cell division is explicitly considered in (c) and (d) with $T_{\mathrm{cell}}=10$ and $\sigma^2_{\mathrm{cell}}=3$. Cell was divided into two daughter cells at time designated by arrows.

number of protein molecules of $X=10^2$, on the other hand, the order of protein number change is chaotically disturbed, resulting in the incoherent oscillation. In this way the degree of persistence of the coherent oscillation depends largely on parameters such as the typical number of proteins in the model. In both $K=1$ and $K=10$ cases we can see that the extrinsic noise does not play a significant role to determine the coherence in oscillation.

The degree of persistence of the oscillatory phase can be quantitatively measured by defining phase coherence, ξ, which is defined in the following way: First, a vector $\mathbf{N}(t)$ is defined by $\mathbf{N}(t)=n_1(t)\mathbf{e}_1+n_2(t)\mathbf{e}_2+n_3(t)\mathbf{e}_3$, where $\mathbf{e}_1=(0,1)$, $\mathbf{e}_2=(\sqrt{3}/2,-1/2)$, and $\mathbf{e}_3=(-\sqrt{3}/2,-1/2)$ are unit vectors on the two-dimensional plane and $n_i(t)$ is the number of the ith protein molecules at time t [see Fig. 5 for the definition of $\mathbf{N}(t)$]. Then, we define the phase angle $\phi(t)$ between $\mathbf{N}(t)$ and $\mathbf{N}(t+\tau)$. τ should be much smaller than the oscillation period but should be larger than the fast noisy fluctuations. We take $\tau=0.1k^{-1}$. $\phi(t)>0$ when the oscillation proceeds, keeping the correct order of expression of proteins. ξ is defined by

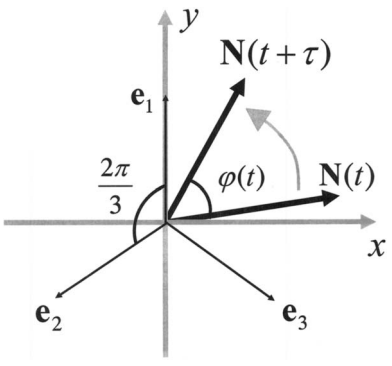

FIG. 5. Schematic explanation of definition of phase coherence ξ.

$$\xi=\frac{2\sum_i \theta(\phi(t))\phi(t)}{\sum_i |\phi(t)|}-1, \tag{8}$$

where θ is a step function, $\theta(\phi)=1$ when $\phi(t)>0$, and $\theta(\phi)=0$ when $\phi(t)\leqslant 0$, and sums are taken over the time steps along the trajectory. $\xi\approx 0$ when $\mathbf{N}(t)$ moves randomly without coherence. ξ increases as the regularity in the oscillation increases and approaches 1 when the oscillation is most coherent. In the following part of this paper we restrict our discussion to the models in which cell division is not explicitly considered and focus on analyzing the intrinsic mechanism of oscillation by using phase coherence introduced in Eq. (8).

B. Adiabaticity, protein number, and leakage rate

As a base line model we first consider the oscillator of $K=1$ without taking account of cell division. In Fig. 6 ξ is plotted in the ω-X plane for different leakage rates with $1-\delta X^m=0(\gamma_0=0)$, $1-\delta X^m=0.02(\gamma_0=\gamma_1/100)$, and $1-\delta X^m=0.18(\gamma_0=\gamma_1/10)$. In the case of $1-\delta X^m=0$, ξ increases as X becomes larger, showing that the coherent oscillation is sustained only when the fluctuation is suppressed with a large enough number of protein molecules. It is interesting to see that there are two regions of large ξ in the ω-X plane. A major region is the one with large ω and X, which we refer to as the adiabatic oscillatory region. A minor region with the fairly large ξ is found in the strongly nonadiabatic region of $\omega<1$, which we refer to as the nonadiabatic oscillatory region. Examples of simulated trajectories in both regions are shown in the right part of Fig. 6.

With increasing leakage rate from $1-\delta X^m=0.02$ to 0.18, ξ becomes smaller. When $1-\delta X^m=0.02$, most coherent os-

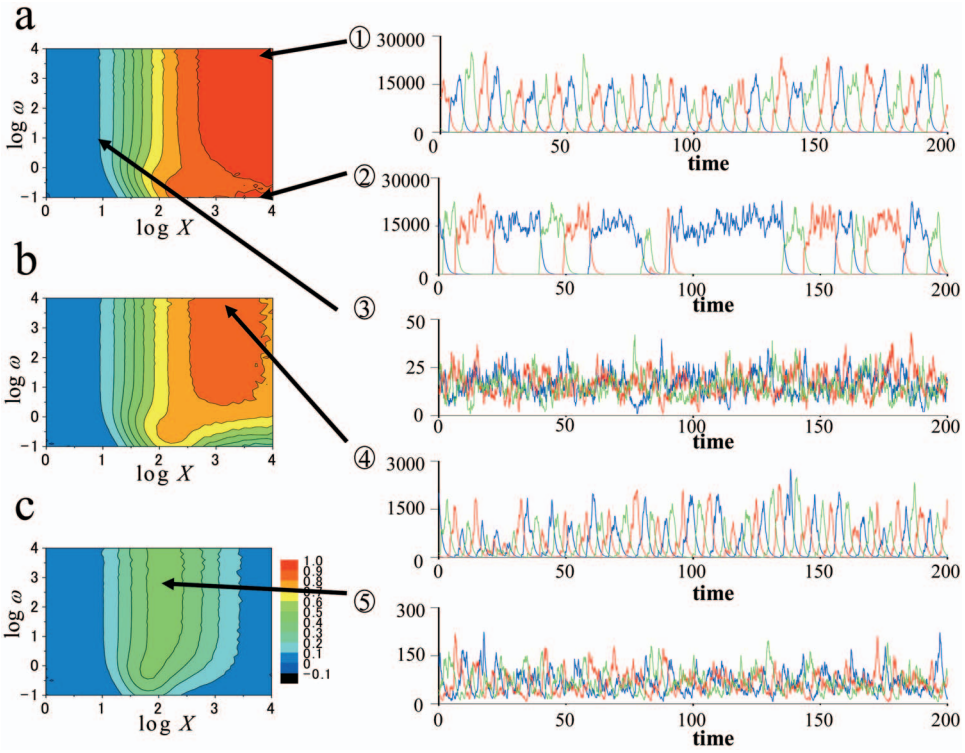

FIG. 6. (Color) Phase coherence ξ is plotted with contour lines in the ω-X plane. ξ increases from blue to red. $K=1$, $X^m=1$, and $X^{eq}=10^3$. (a) $1-\delta X^m=0$, (b) $1-\delta X^m=0.02$, and (c) $1-\delta X^m=0.18$. Trajectories are exemplified for parameter values (1) $X=10^{3.9}$ and $\omega=10^{-1}$, (2) $X=10^{3.9}$ and $\omega=10^{3.9}$, and (3) $X=10^2$ and $\omega=10^2$ for (a), (4) $X=10^3$ and $\omega=10^{3.9}$ for (b), and $X=10^2$ and $\omega=10^{2.9}$ for (c). Time is measured in units of k^{-1}.

cillation is observed in the region of moderate X. This is because with too large X with finite $1-\delta X^m$ the protein number does not decrease enough in the DNA off state and hence the phase coherence in the oscillation is disturbed: The large X should assure the applicability of the law of large number, but in the case of finite leakage rate the large X destroys the coherence in oscillation. When $1-\delta X^m=0.18$, ξ is small everywhere in the ω-X plane and the region of relatively large ξ is located at the region of smaller X. Both in cases of $1-\delta X^m=0.02$ and $1-\delta X^m=0.18$, the region of the relatively large ξ is only at large ω, and, in contrast with the case of $1-\delta X^m=0$, there is no region of large ξ in the strongly nonadiabatic regime.

Since the strength of noise is decisively affected by ω and X, results of Fig. 6 show that oscillation is coherent when the strength of noise is tuned to be within certain ranges. Such effect of noise with the chosen strength has been observed in many oscillatory or excitable systems and is called autonomous stochastic resonance, or coherent resonance.[29] In statistical analyses of coherent resonance, various quantities have been used to measure the coherence of oscillation: signal-to-noise ratio,[30–32] number of adjacent spikes,[33,34] coefficient of variation,[29,35] effective diffusion coefficient,[29] and kurtosis of suitable quantities[36] are examples. Denoting the time length between adjacent oscillatory peaks of $n_1(t)$ by T, we here calculate the kurtosis $K_T=\langle(T-\langle T\rangle)^4\rangle/\langle(T-\langle T\rangle)^2\rangle-3.0$, coefficient of variation $R_{CV}=\sqrt{\langle(T-\langle T\rangle)^2\rangle}/\langle T\rangle$, and effective diffusion coefficient $D_{eff}=\langle(T-\langle T\rangle)^2\rangle/2\langle T\rangle^3$, where $\langle\cdots\rangle$ is an average taken along trajectories. In Fig. 7 we show K_T, R_{CV}, and D_{eff} for the case of $1-\delta X^m=0$. It should be noted that K_T, R_{CV}, and D_{eff} can be defined only when the oscillatory peaks of $n_1(t)$ are not buried in the chaotic random modulations, so that only the results for the region of a relatively large ξ, the results for $\log_{10}X>3$, are shown in Fig. 7. Comparing Figs. 6(a) and 7, we find that K_T is large in adiabatic and nonadiabatic oscillatory regions. The large K_T with $K_T>0$ in these regions implies that the distribution of T is narrower than Gaussian reflecting the coherence in oscillation. R_{CV} is small in the adiabatic oscillatory region, so that the coherence in the nonadiabatic region is not captured by R_{CV} but both the co-

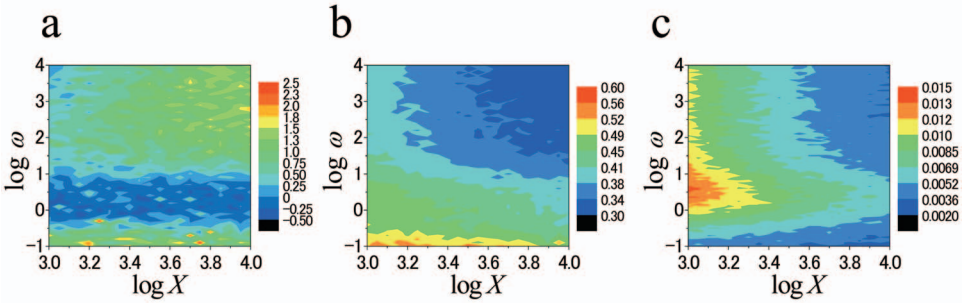

FIG. 7. (Color) Other comparable statistical quantities to measure the phase coherence. (a) Kurtosis K_T, (b) coefficient of variation R_{CV}, and (c) effective diffusion coefficient D_{eff} are plotted in the ω-X plane. $1-\delta X^m=0$, $K=1$, $X^m=1$, and $X^{eq}=10^3$.

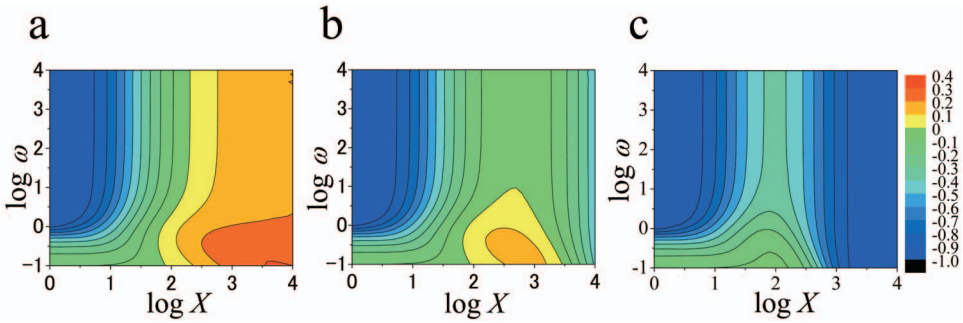

FIG. 8. (Color) Stability of the stationary solution of the mean-field equation. The largest eigenvalue, $\eta_{\max}$, in the linear stability analysis of the stationary solution is plotted in the ω-X plane. $K=1$, $X^m=1$, and $X^{\mathrm{eq}}=10^3$. (a) $1-\delta X^m=0$, (b) $1-\delta X^m=0.02$, and (c) $1-\delta X^m=0.18$. In the region colored from yellow to red with $\eta_{\max}>0$, the stationary solution is unstable against the oscillation.

herence in the adiabatic oscillatory region and that in the nonadiabatic oscillatory region are represented by small values of D_{eff}.

C. Constructive role of noise

Light is shed on the effects of stochasticity by comparing the above numerical results with the lowest order mean-field description of Eq. (6). Equation (6) has a stationary solution of $C_{i,p}=C$, $M_{i,p,1}=M_1$, $M_{i,p,0}=M_0$, and $N_i=N$. This solution becomes unstable when the oscillatory solution appears. The linear stability analysis was performed by expanding variables in Eq. (6) around the stationary solution as $C_{i,p}=C+\delta C_{i,p}$, $M_{i,p,1}=M_1+\delta M_{i,p,1}$, $M_{i,p,0}=M_0+\delta M_{i,p,0}$, and $N_i=N+\delta N_i$ up to the lowest order terms. The linear stability of the stationary solution is examined by writing $\delta C_{i,p}\sim\delta M_{i,p,1}\sim\delta M_{i,p,0}\sim\delta N_i\sim\exp(\eta t)$ to derive the secular equation. We then have a spectrum of η, in which the largest η is denoted by $\eta_{\max}$. The stationary state is stable when $\eta_{\max}<0$. When $\eta_{\max}=0$, the solution of Eq. (6) shows the Hopf bifurcation from the stationary solution to the limit cycle, and when $\eta_{\max}>0$, the stationary state becomes unstable and is replaced by the oscillatory solution. In Fig. 8 $\eta_{\max}$ is plotted in the ω-X plane. In the case of $1-\delta X^m=0$ the region of $\eta_{\max}>0$ roughly coincides with the region of large ξ in Fig. 6, showing that the lowest order mean-field method gives a good prediction for the condition of oscillation. There is a difference between two results that the strongly nonadiabatic region has the largest $\eta_{\max}$ in Fig. 8 but ξ is larger in the adiabatic oscillatory region in Fig. 6. This difference becomes significant in the case of the finite leakage rate with $1-\delta X^m\neq 0$. In the case of $1-\delta X^m=0.02$ the lowest order mean-field method predicts that the oscillatory solution appears only in the strongly nonadiabatic region, as shown in Fig. 8, but ξ is large only in the weakly adiabatic or adiabatic region, as shown in Fig. 6. In the weakly adiabatic or adiabatic regime, the stationary solution is stable in Eq. (6) but is destabilized by the stochastic fluctuation in numerical simulation, which should lead the trajectories to the oscillatory behavior. This is an example of noise-induced bifurcations which have been discussed in many contexts of chemical physics and biophysics.[37,38] In the strongly nonadiabatic regime, on the other hand, the lowest order mean-field method predicts the appearance of the oscillatory solution. In the numerical simulation the stationary state is not stable due to the large fluctuation but the protein number is so much influenced by the stochastic DNA state fluctuation, which destroys the phase coherence in the nonadiabatic region except for the case of $1-\delta X^m=0$.

In Fig. 9 the amplitude of stochastic fluctuations of the number of mRNA molecules is evaluated by a Fano factor, $\sigma^2_{m(1,0,0)}/M_{100}$, where $\sigma^2_{m(1,0,0)}$ and M_{100} are the dispersion and the average of the mRNA number at the particular switching state, $S_1=1$, $S_2=0$, and $S_3=0$; $\sigma^2_{m(1,0,0)}=\Sigma_{(S,m,n)}\times(m_1)^2S_1(1-S_2)(1-S_3)P(\{S_i\},\{m_{i,p}\},\{n_i\})-(M_{100})^2$; and $M_{100}=\Sigma_{(S,m,n)}m_1S_1(1-S_2)(1-S_3)P(\{S_i\},\{m_{i,p}\},\{n_i\})$. One can find that the Fano factor is larger than 1 roughly around the region where ξ is large, which is consistent with the observation that the mRNA distribution deviates from Poissonian

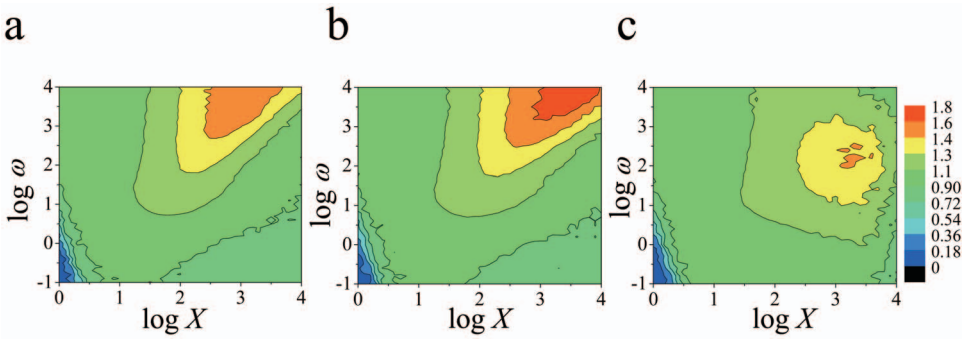

FIG. 9. (Color) The Fano factor of the protein number fluctuation in a specific DNA state, $S_1=1$, $S_2=0$, and $S_3=0$, is plotted with contour lines in the ω-X plane. The Fano factor increases from blue to red. $K=1$, $X^m=1$, and $X^{\mathrm{eq}}=10^3$. (a) $1-\delta X^m=0$, (b) $1-\delta X^m=0.02$, and (c) $1-\delta X^m=0.18$.

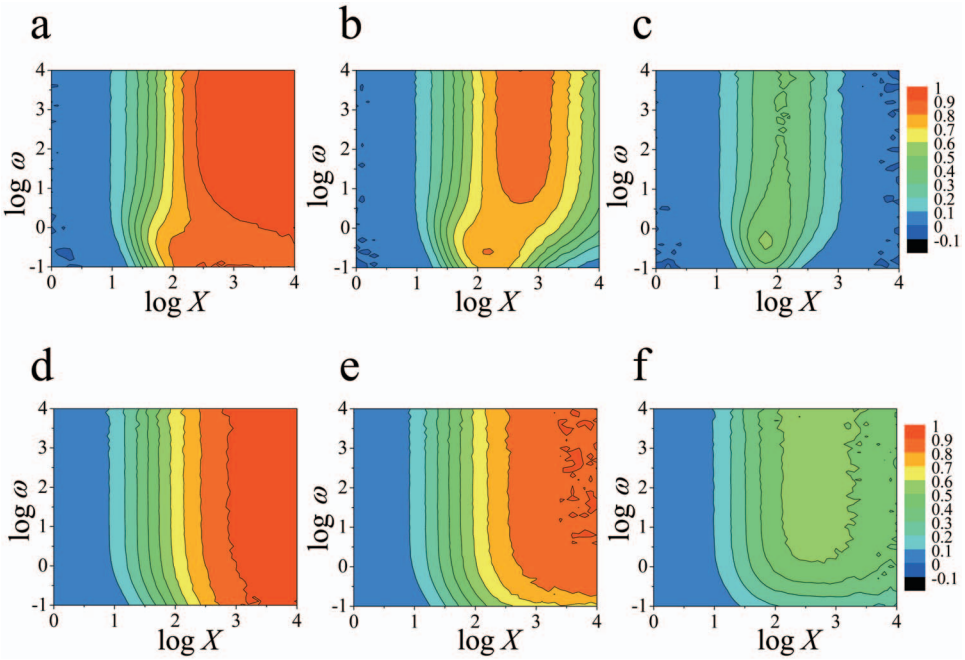

FIG. 10. (Color) Phase coherence ξ for the case of large production rate of mRNA with $X^m=10$ [(a)–(c)] and for the case of small production rate of mRNA with $X^m=0.1$ [(d)–(f)] is plotted with contour lines in the ω-X plane. In the case of $X^m=0.1$ proteins are produced as bursts. $K=1$ and $X^{eq}=10^3$. (a) $1-\delta X^m=0$, (b) $1-\delta X^m=0.02$, (c) $1-\delta X^m=0.18$, (d) $1-\delta X^m=0$, (e) $1-\delta X^m=0.02$, and (f) $1-\delta X^m=0.18$.

in the region where the lowest order mean-field description becomes not applicable, so that the oscillation is assisted by the stochastic fluctuation beyond Poissonian.

D. Bursts in translation

Bursting in protein production has been regarded as one of the major source of noise in prokaryotes.[39] Proteins are produced in bursts when the average number of mRNA is small in the cell. This corresponds to the small X^m case in the present model. ξ for $X^m=10$ and ξ for $X^m=0.1$ are compared in Fig. 10. Results for $X^m=10$ are similar to those for $X^m=1$ shown in Fig. 6. Results in the case of $X^m=0.1$ are, however, fairly different from those of $X^m=1$, showing that the effects of bursts in translation become evident only when the typical number of mRNA molecules, X^m, is smaller than 1. Especially in the case of $1-\delta X^m=0.02$ with $X^m=0.1$ the region of large ξ extends toward the large X direction: Fluctuation induced by bursts suppresses the effects of the leakage in protein production in the DNA off state. This is another aspect of the constructive role of stochasticity.

IV. COLLECTIVE DYNAMICS IN COUPLED GENE OSCILLATORS

In a usual experimental setup, multiple copies of plasmids with $K>1$ are introduced in a cell at the same time. In Fig. 11 ξ is shown for $K=3$ and 10 in the ω-X plane. In the case of $1-\delta X^m=0$ the region of large ξ shown in Fig. 11 is enlarged from that for $K=1$ of Fig. 6. This enlargement of the large ξ region implies that the cooperative interactions among multiple repressilators enhance the coherence in os-

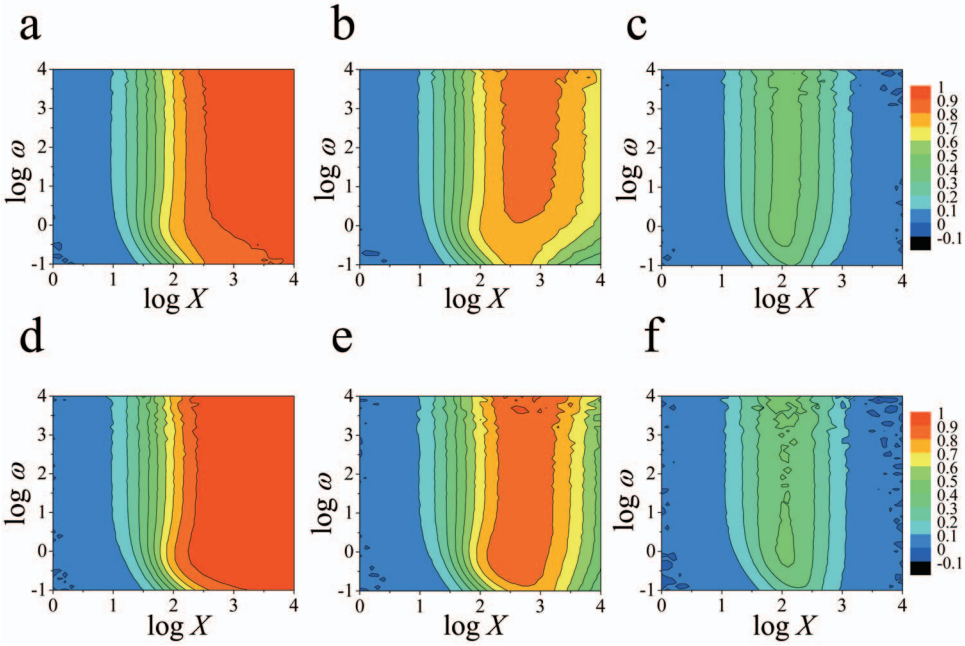

FIG. 11. (Color) Phase coherence ξ for the multiply coupled repressilators is plotted with contour lines in the ω-X plane. $X^m=1$ and $X^{eq}=10^3$: (a) $1-\delta X^m=0$ and $K=3$, (b) $1-\delta X^m=0.02$ and $K=3$, (c) $1-\delta X^m=0.18$ and $K=3$, (d) $1-\delta X^m=0$ and $K=10$, (e) $1-\delta X^m=0.02$ and $K=10$, and (f) $1-\delta X^m=0.18$ and $K=10$.

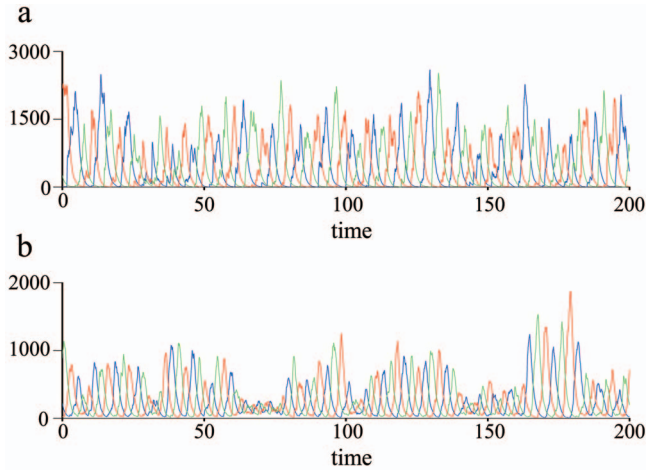

FIG. 12. (Color) Examples of trajectories of the multiply coupled repressilators with parameter values $X^m=1$ and $X^{eq}=10^3$, $X=10^3$ and $\omega=10^{2.9}$. (a) $K=1$ and (b) $K=10$. Time is measured in units of k^{-1}.

cillation. In the case of $1-\delta X^m=0.02$ the region of large ξ for $K=3$ and 10 is elongated toward the nonadiabatic regime, but the region is narrowed at the large X side from the region for $K=1$. In other words, suppression of coherence arising from the leakage production of proteins is emphasized by the decrease in noise due to the coupling of multiple repressilators.

Example trajectories are shown in Fig. 12. We can see that the oscillation period is shortened by about 30% due to the coupling of ten oscillators. An interesting observation is that a fluctuation which was not so evident in a single repressilator is found more evidently in multiple repressilators: The peak number of protein molecules fluctuates along the trajectory. In other words, fluctuation in amplitude of the oscillation is large in the coupled oscillator systems although the oscillation phase proceeds coherently with a large ξ. This amplitude fluctuation implies that the coupled multiple repressilators are not perfectly synchronized to each other: When some of the K repressilators have delayed or advanced phases, the sum of expressed proteins should fluctuate, resulting in the amplitude fluctuation in the protein number oscillation.

The correlation among repressilators is estimated by the correlation among the DNA states, R, defined by

$$R^{\mathrm{DNA}}=\frac{2}{K(K-1)}\sum_{(p,q)}(\langle S_{i,p}S_{i,q}\rangle-\langle S_{i,p}\rangle\langle S_{i,q}\rangle), \tag{9}$$

where $\langle\ldots\rangle$ is the average taken along the simulated trajectories and $\Sigma_{(p,q)}$ denotes the summation over the plasmid pairs. From the symmetry in each repressilator, R^{DNA} does not depend on i. R^{DNA} is shown in Figs. 13(a) and 13(b). R^{DNA} is largest at the weakly adiabatic regime of $\omega\approx 1$. For $\omega<1$, R^{DNA} is small because of the loss of phase coherence in each repressilator, and for $\omega>1$, R^{DNA} is reduced because the protein number changes more slowly than the DNA state and only the time averaged DNA state is relevant in oscillation. $\langle S_{i,p}\rangle\approx 0.33$ from the symmetry of the system. When repressilators in different plasmids are perfectly synchronized, $\langle S_{i,p}S_{i,q}\rangle$ must be around 0.33, which makes $R^{\mathrm{DNA}}\approx 0.22$. The largest value of R^{DNA} in Figs. 13(a) and 13(b) is about half or less than half of this idealized value, implying that the coupled multiple repressilators show a considerable amount of desynchronization, which should lead to the amplitude fluctuation in the protein number oscillation. In Figs. 13(c) and 13(d) the correlation among the mRNA numbers, R^{RNA}, are shown,

$$R^{\mathrm{RNA}}=\frac{2}{K(K-1)}\sum_{(p,q)}(\langle m_{i,p}m_{i,q}\rangle-\langle m_{i,p}\rangle\langle m_{i,q}\rangle). \tag{10}$$

Figures 13(c) and 13(d) show that the mRNA number faithfully follows the fluctuation of the DNA state to become the source of the amplitude fluctuation in the protein numbers.

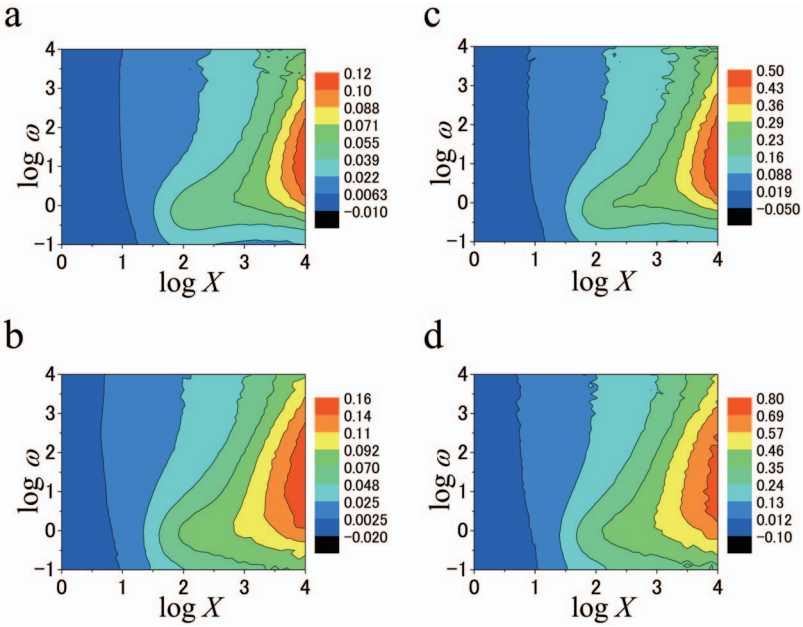

FIG. 13. (Color) Correlations for the DNA state and the mRNA number among multiple repressilators. (a) Correlation among the DNA states of $K=3$ repressilators, (b) correlation among the DNA states of $K=10$ repressilators, (c) correlation among the mRNA numbers of $K=3$ repressilators, and (d) correlation among the mRNA numbers of $K=10$ repressilators.

V. SUMMARY AND DISCUSSION

In this paper effects of factors which have been regarded as important in determining the properties of fluctuating gene switches were examined in the dynamically oscillating gene circuit. A rich variety of responses of dynamical properties to those factors were found.

For a single isolated repressilator the mean-field description derived under the assumption of the Poisson distribution of molecular numbers predicts the oscillatory behavior almost correctly when the leakage production rate is strongly suppressed to be $1-\delta X^m=0$. There is, however, a large difference between the mean-field prediction and the exact numerical results when the leakage rate is finite: The mean-field prediction suggested that the oscillatory coherence is not robust against the small increase of the leakage rate. The exact numerical results, on the other hand, showed the robust oscillatory behavior against the small increase in the leakage rate in the weakly adiabatic and adiabatic regions, which implies that the repressilator undergoes a noise-induced bifurcation from the stationary state to the oscillatory state. With the finite leakage rate the coherent oscillation is disturbed when the product protein number is large. This disruption of coherence due to the leakage production is suppressed by the stochastic fluctuation generated by bursts in translation but is enhanced by the coupling of multiple repressilators. Thus, the noise generated in the transcription or translation process should have both two faces, one to destruct the coherent persistent oscillation through the chaotic randomization and the other to help the coherent oscillation by destabilizing the stationary state or by decreasing the systematic tendency of suppressing the oscillation with the finite leakage rate.

When multiple repressilators are coupled to each other, the coherence in the oscillatory phase is enhanced, but there appears fluctuation in the amplitude of oscillation. The amplitude fluctuation is due to the fluctuating synchronization and desynchronization of DNA states in multiple repressilators. It should be interesting to further analyze the amplitude fluctuation to examine the applicability of the "mode" concept in this many-body dynamics.

These results obtained for a single and coupled multiple oscillators should help to design experiments. For example, the phase coherence may be able to be controlled through modulation in adiabaticity. Adiabaticity can be modulated by changing the binding affinity of repressors to promoter or by changing the degradation rate of repressors. Bursts in translation can be controlled by changing the concentration of ribosome in a cell, and it should be possible to examine the prediction of the present model on whether the bursting can compensate for the phase disturbance arising from the finite leakage rate of protein production. It is also interesting to examine the role of multiple gene circuits by changing the number of plasmids in a cell. By controlling the number of plasmids in a cell we will be able to control both the phase fluctuation and the amplitude fluctuation in oscillation. There are an abundance of examples of duplicated or multiplicated genes in individual genomes. Enhancement of phase coherence through cooperative interactions among those genes might be an evolutionary reason for the multiplication of genes in a genome.

The usefulness of theoretical models and numerical simulations to design gene circuits has been recognized through recent synthetic biological experiments. In this paper factors which significantly control the fluctuation in gene switches are examined in a systematic numerical observation to see their effects on the genetic oscillatory dynamics. A rich variety of responses of oscillatory dynamics to noisy fluctuations were found, which showed that constructing models of dynamically oscillating gene circuits should enlarge the possibility of designing further synthetic experiments and to give deeper insights on the biological design architecture.

ACKNOWLEDGMENTS

This work was supported by grants from the Ministry of Education, Culture, Sports, Science, and Technology, Japan and from Japan Society for Promotion of Science and by grants for the 21st century COE program for Frontiers of Computational Science.

[1] M. B. Elowitz and S. Leibler, Nature (London) **403**, 335 (2000).
[2] T. S. Gardner, C. R. Cantor, and J. J. Collins, Nature (London) **403**, 339 (2000).
[3] F. J. Isaacs, J. Hasty, C. R. Cantor, and J. J. Collins, Proc. Natl. Acad. Sci. U.S.A. **100**, 7714 (2003).
[4] M. B. Elowitz, A. J. Levine, E. D. Siggia, and P. S. Swain, Science **297**, 1183 (2002).
[5] E. M. Ozbudak, M. Thattai, H. N. Lim, B. I. Shraiman, and A. van Oudenaarden, Nature (London) **427**, 737 (2004).
[6] J. Yu, J. Xiao, X. Ren, K. Lao, and X. S. Xie, Science **311**, 1600 (2006).
[7] N. J. Guido, X. Wang, D. Adalsteinsson, D. McMillen, J. Hasty, C. R. Cantor, T. C. Elston, and J. J. Collins, Nature (London) **439**, 856 (2006).
[8] M. Kærn, T. C. Elston, W. J. Blake, and J. J. Collins, Nat. Rev. Genet. **6**, 451 (2005).
[9] A. M. Walczak, J. N. Onuchic, and P. G. Wolynes, Proc. Natl. Acad. Sci. U.S.A. **102**, 18926 (2005).
[10] T. B. Kepler and T. C. Elston, Biophys. J. **81**, 3116 (2001).
[11] J. E. M. Hornos, D. Schultz, G. C. P. Innocentini, J. Wang, A. M. Walczak, J. N. Onuchic, and P. G. Wolynes, Phys. Rev. E **72**, 051907 (2005).
[12] R. Bundschuh, F. Hayot, and C. Jayaprakash, Biophys. J. **84**, 1606 (2003).
[13] R. Gunawan, Y. Cao, L. Petzold, and F. J. Doyle III, Biophys. J. **88**, 2530 (2005).
[14] P. B. Warren and P. R. ten Wolde, Phys. Rev. Lett. **92**, 128101 (2004).
[15] P. B. Warren and P. R. ten Wolde, J. Phys. Chem. B **109**, 6812 (2005).
[16] A. M. Walczak, M. Sasai, and P. G. Wolynes, Biophys. J. **88**, 828 (2005).
[17] T. Ushikubo, W. Inoue, M. Yoda, and M. Sasai, Chem. Phys. Lett. **430**, 139 (2006).
[18] M. Sasai and P. G. Wolynes, Proc. Natl. Acad. Sci. U.S.A. **100**, 2374 (2003).
[19] J. M. Raser and E. K. O'Shea, Science **304**, 1811 (2004).
[20] A. Becskei, B. Seraphin, and L. Serrano, EMBO J. **20**, 2528 (2001).
[21] D. T. Gillespie, J. Phys. Chem. **81**, 2340 (1977).
[22] H. H. McAdams and A. Arkin, Proc. Natl. Acad. Sci. U.S.A. **94**, 814 (1997).
[23] L. Chen, R. Wang, T. J. Kobayashi, and K. Aihara, Phys. Rev. E **70**, 011909 (2004).
[24] L. M. Tuttle, H. Sallis, J. Tomshine, and Y. N. Kaznessis, Biophys. J. **89**, 3873 (2005).
[25] J. M. G. Vilar, H. Y. Kueh, N. Barkai, and S. Leibler, Proc. Natl. Acad. Sci. U.S.A. **99**, 5988 (2002).
[26] J. Garcia-Ojalvo, M. B. Elowitz, and S. H. Strogatz, Proc. Natl. Acad. Sci. U.S.A. **101**, 10955 (2004).
[27] M. B. Elowitz, M. G. Surette, P.-E. Wolf, J. B. Stock, and S. Leibler, J. Bacteriol. **181**, 97 (1999).

[28] E. Aurell, S. Brown, J. Johanson, and K. Sneppen, Phys. Rev. E **65**, 051914 (2002).
[29] B. Linder, J. García-Ojalovo, A. Neiman, and L. Schimansky-Geiger, Phys. Rep. **392**, 321 (2004).
[30] A. Guderian, G. Dechert, K.-P. Zeyer, and F. W. Schneider, J. Phys. Chem. **100**, 4437 (1996).
[31] A. Förster, M. Merget, and F. W. Schneider, J. Phys. Chem. **100**, 4442 (1996).
[32] Y. Jiang, S. Zhong, and H. Xin, J. Phys. Chem. A **104**, 8521 (2000).
[33] T. Amemiya, T. Ohmori, M. Nakaiwa, and T. Yamaguchi, J. Phys. Chem. A **102**, 4537 (1998).
[34] T. Amemiya, T. Ohmori, T. Yamamoto, and T. Yamaguchi, J. Phys. Chem. A **103**, 3451 (1999).
[35] A. Pikovsky and J. Kurths, Phys. Rev. Lett. **78**, 775 (1997).
[36] A. Lemarchand and B. Nowakowski, Europhys. Lett. **71**, 530 (2005).
[37] W. Horshemke and R. Lefever, *Noise-Induced Transitions* (Springer, Berlin, 1984).
[38] A. Lemarchand and B. Nowakowski, Physica A **331**, 409 (2004).
[39] E. M. Ozbudak, M. Thattai, I. Kurtser, A. D. Grossman, and A. van Oudenaarden, Nat. Genet. **31**, 69 (2002).